14017

Femtosecond Aqueous Solvation at a Positively Charged Surfactant/Water Interface

Alexander V. Benderskii,[†] **Joel Henzie, Saonli Basu, Xiaoming Shang, and Kenneth B. Eisenthal***

Department of Chemistry, Columbia University, New York, New York 10027

Received: February 27, 2004

The effect of a positively charged dodecyl trimethylammonium bromide (DTAB) surfactant on the aqueous solvation of coumarin 314 (C314), a solvatochromic molecule, at the air/water interface was investigated. Steady-state and femtosecond time-resolved second harmonic generation (SHG) spectroscopy was employed as a surface-selective tool to characterize the solvation of C314. The molecular orientation and the static and dynamic solvation of the probe C314 at the positively charged surfactant interface were found to be significantly different from that at the previously studied neat air/water interface and at a negatively charged surfactant air/water interface. Steady-state SHG spectra show a red shift and therefore increased local polarity at the positively charged interface (λ_{max} = 436 nm) compared to the negatively charged interfaces (λ_{max} = 431–432 nm) and the surfactant-free air/water interface (λ_{max} = 423 nm), though less polar than bulk water (448 nm). Two diffusive dynamical time scales τ_1 and τ_2 of aqueous solvation were obtained at the DTAB interfaces, as is the case at air/water, at negatively charged surfactant interfaces, and in bulk water. Both the solvation times and their relative amplitudes change as a function of the positively charged surfactant surface coverage. As the DTAB surface density increases from 500 Å^2/molecule to 100 Å^2/molecule, the fast component τ_1 slows from 380 to 550 fs, whereas the amplitude of the slower solvation component τ_2 is reduced to almost zero. This is significantly different from the behavior observed at the negatively charged surfactant interfaces.

Introduction

Surfaces of biomembranes host many fundamental biological processes including electron transfer, energy transduction, biosynthesis, and molecular recognition.[1] Solvent properties of water near these interfaces profoundly affect both the energetics and the dynamics of chemical reactions at these surfaces. For example, the dynamics of solvation can be a rate-limiting step in interfacial electron transfer.[2] Due to the interactions with the multitude of interfacial moieties present at a biological interface, properties of water near the interface may be drastically different from bulk water. In fact, the term "biological water" has been coined to describe a thin layer of water adjacent to biological structures such as cell membranes, organelles, and proteins.[3,4] In a series of previous publications, we have focused on the static and dynamic solvation at model interfaces, monolayers of neutral[5] and anionic surfactants at the air/water interface.[6,7] In the present study, we investigate the effect of the positively charged surfactant monolayer on the aqueous solvation of the same probe dye molecule, coumarin 314. This allows a direct comparison of the effects of positively versus negatively charged surfactants on the process of aqueous solvation. Considering electrostatic forces, the oppositely charged surfactants will tend to orient interfacial water molecules in opposite directions. The negatively charged surfactant favors the water molecules to be in the "hydrogen up" direction,[8,9] opposite to the preferred water orientation at the air/water interface, where the majority of hydrogens point down perpendicular to the surface.[10–12] On the contrary, the positively charged surfactant tends to orient the water molecules "oxygens up",[8,9] i.e., in the same direction of the preferred water orientation as at the air/water interface. Thus,

in the aqueous region between the surfactant headgroups the orientation of water molecules is preferentially oriented opposite to water molecules immediately neighboring the anionic surfactant headgroup versus the same preferred orientation for the cationic surfactant headgroup. Besides the electrostatic interaction of the positively versus the negatively charged surfactant with water molecules, its interactions with the permanent dipole moment of C314 would align the C314 molecules in the opposite direction.

Monolayers of lipid surfactants present a convenient model system which can be used to mimic the chemical composition and electric charge of the more complex biomembrane surfaces, while allowing a high degree of control over the experimental conditions. Surfactants with a chosen headgroup may be used to selectively study the effects of the chemical functionalities present at the interface. Surface charge density can be systematically altered by adjusting the surface coverage and, in some cases, by controlling the ionization state of the headgroup by adjusting the pH of the aqueous phase. In our previous studies, two anionic surfactants were used, i,.e., sodium dodecyl sulfate, SDS $CH_3(CH_2)_{11}O–SO_3{}^-–Na^+$, and the negative form of stearic acid, $CH_3(SH_2)_{16}COO^-$. The surfactant used in this study is a cationic one, dodecyltrimethylammonium bromide, DTAB, $CH_3(CH_2)_{11}–N^+(CH_3)_3–Br^-$.

Two aspects characterize the process of solvation. Static solvation describes the equilibrium energy stabilization of a solute by interactions with the surrounding solvent molecules. In the case of dipolar solute and solvent molecules (as in the present study), this energy is often dominated by the electrostatic dipole–dipole interactions and specific interactions such as hydrogen bonding. The response of the solvent to a solute charge redistribution is not instantaneous and is referred to as solvation dynamics. For the dipolar aqueous solvation, this relaxation

† Present address: Department of Chemistry, Wayne State University, Detroit, MI 48202.

dynamics involves orientational and translational motions of the water molecules, and associated rearrangements of the aqueous hydrogen bond network. Bulk water is characterized by 3 characteristic solvation time scales. The so-called inertial component is within a $\tau \sim 25-30$ fs range[13-15] and arises from unhindered librations of water. The two "diffusive" components have characteristic times $\tau_1 = 130-250$ fs and $\tau_2 = 0.69-1.2$ ps and are due to the rearrangement of the hydrogen bond network, i.e., breaking and making water–water H-bonds.[13-15]

At both the air/water and surfactant air/water interfaces, two diffusive solvation times have been observed using femtosecond time-resolved second harmonic generation (TRSHG). This surface-selective spectroscopic tool provides a way to focus only on the probe molecules adsorbed at the interface, with no contribution from the bulk phase. Previously, it has been found that τ_1 and τ_2 depend on the surface density of the anionic surfactant.[6] Here, we demonstrate that, despite some qualitative similarities, the behavior of the two diffusive time scales τ_1 and τ_2 as a function of the positively charged surfactant coverage is different from the negatively charged surfactant case. The orientation of the probe molecule and its static solvation are also found to be different at the oppositely charged interfaces.

In general, three types of interactions may affect the molecular structure and dynamics near the interface: (1) long-range electrostatic interactions of water dipoles with the field of the charged planar surface and interactions of the dipolar probe molecule with water dipoles and with the charged interface, (2) short-range chemically specific interactions such as hydrogen bonding between water molecules and the surfactant headgroup moieties (e.g., $CH_3(CH_2)_{11}-SO_4^-$), and (3) hydrophobic interaction of the surfactant headgroup (e.g., methyl groups of DTAB) with water molecules. The discovered differences between the effects caused by cationic versus anionic headgroups at the aqueous interfaces indicate the asymmetry of the water response with respect to the sign of the applied electric field and point to the importance of specific local interactions such as hydrogen bonding of the sulfate headgroup of SDS with interfacial water molecules in contrast with the hydrophobic interactions of the trimethylammonium headgroup of DTAB with surrounding water molecules.

Experimental Section

Saturated aqueous solutions of laser grade coumarin 314 (Acros) were prepared in deionized double-distilled water by sonicating, heating and stirring for 2 h, and then allowing the solution to equilibrate to room temperature for at least 3 h. The bulk dye concentration $C = 15\ \mu M$ was obtained from the UV–vis absorption spectroscopy using the molecular extinction coefficient of C314.[16] Dodecyl trimethylammonium bromide (DTAB) was purchased from Aldrich (98%+ purity) and was used without further purification. Its molecular structure together with C314 is schematically shown here.

Coumarin 314
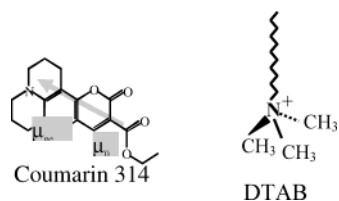
DTAB

The arrows in C314 show the permanent dipole moment μ_0 and the transition dipole moment of the S_0 to S_1 transition μ_{ge} ($=\mu_e - \mu_g$). DTAB is a water-soluble surfactant that readily forms positively charged monolayer films. The surface coverage
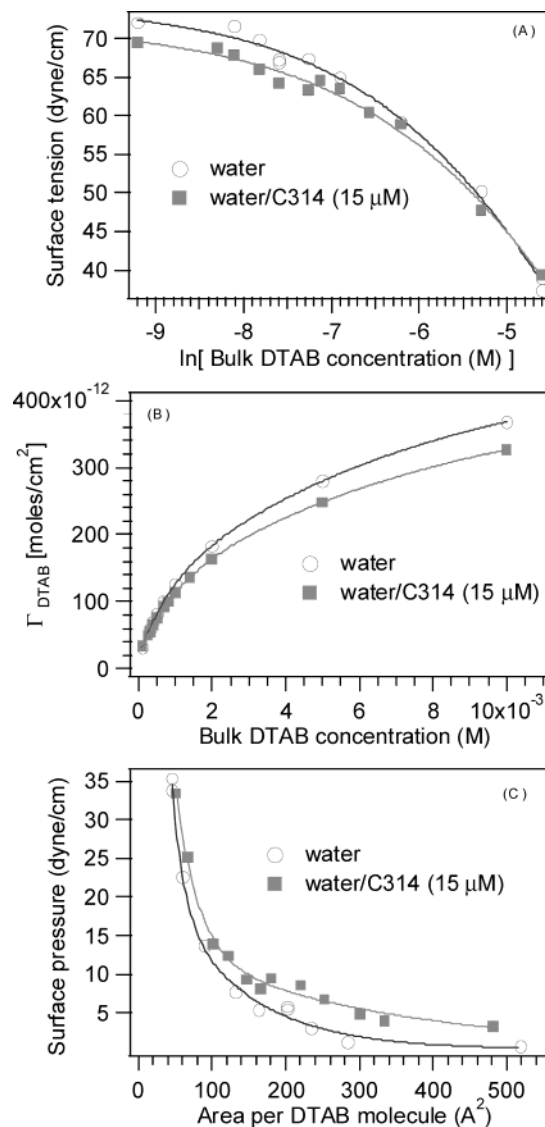

Figure 1. (A) Surface tension of dodecyl trimethylammonium bromide (DTAB) solutions in water (○) and in 15 μM coumarin 314 water solution (■) as a function of DTAB bulk concentration. (B) Surface excess of DTAB as a function of bulk concentration calculated using the Gibbs adsorption isotherm. (C) 2D-phase diagram (surface pressure π vs area per DTAB molecule) of DTAB monolayers on water (○) and on a 15 μM coumarin 314 water solution (■).

is a function of the bulk surfactant concentration, as described by the Gibbs adsorption isotherm

$$\Gamma_{DTAB} = -\frac{1}{2RT}\frac{\partial\gamma}{\partial[\ln C_{DTAB}]} \quad (1)$$

where Γ_{DTAB} is the surface excess of the surfactant, C_{DTAB} is the bulk concentration, and γ is the surface tension. The factor 2 in the denominator reflects adsorption of a completely dissociated ionic surfactant.

A Wilhelmy plate balance was used to measure the surface tension of the aqueous solutions containing a saturated concentration of coumarin 314 and variable concentrations of DTAB. The resultant γ versus $\ln C_{DTAB}$ curves, presented in Figure 1A, were fitted and differentiated using eq 1 to calculate the DTAB surface excess, Figure 1B. As a reference, we also show the surface tension curves in the absence of coumarin 314. The difference between the two curves is due to the adsorption of C314, which is surface active and interacts with the DTAB

Femtosecond Aqueous Solvation

J. Phys. Chem. B, Vol. 108, No. 37, 2004 **14019**
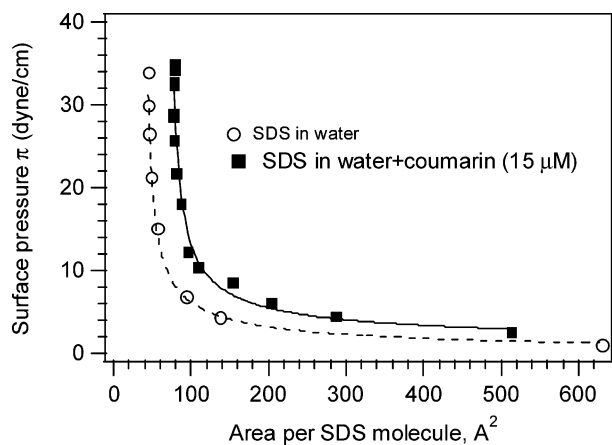
Figure 2. 2D-phase diagram (surface pressure π vs area per SDS molecule) of SDS Gibbs monolayers on water (O) and on a 15 μM coumarin 314 water solution (■).

Figure 3. (■) Effect of the cationic DTAB surfactant on the molecular orientation of coumarin 314 at the air/water interface, as a function of the DTAB surface density. (O) Molecular orientation of coumarin 314 at the anionic SDS surfactant air/water interface.

surfactant and the water organized about the DTAB surfactant. The effect of C314 on the DTAB phase diagram relative to the phase diagram without C314 is shown in Figure 1C. For comparison, Figure 2 shows the phase diagram of SDS with and without C314. It is clear that the effect of C314 on the DTAB phase diagram is different from that on the SDS phase diagram.[6] An explanation of this different behavior is proposed in the Results and Discussion section. Three DTAB bulk concentrations, 0.14, 0.5, and 2.0 mM, corresponding to the surface coverage of 500, 200, and 100 Å^2/DTAB molecule, were chosen for the time-resolved solvation dynamics measurements. Note that all three concentrations are well below the critical micelle concentration (cmc) for DTAB, 14 mM.

A detailed description of the second harmonic generation spectrometer has been presented elsewhere.[5,6] The home-built instrument is based on the regeneratively amplified femtosecond Ti:sapphire laser system (Clark-MXR CPA-1000), which produces 120 fs pulses at a 1 kHz repetition rate. The fundamental wavelength was tuned to 840 nm, and 80% of the output (0.75 mJ/pulse) was used to pump an optical parametric amplifier (Clark-MXR OPA). The idler output of the OPA was frequency doubled in a phase-matched 0.5 mm thick BBO crystal to produce probe pulses of tunable wavelengths. In most of the experiments, a $\lambda_{pr} = 860$ nm probe wavelength was used for second harmonic generation, taking advantage of the two-photon SHG resonance with C314 at the interface. The choice of the SH probe wavelength ($\lambda_{SH} = 430$ nm) with respect to the transition wavelength of the probe molecule at the interface is discussed later. The sample solution was contained in a shallow Teflon beaker. The probe beam (15−20 μJ/pulse) was incident at the sample surface at a 70° angle from the vertical. The reflected second harmonic light generated at the surface of the solution was collected using two lenses, spectrally filtered from the fundamental frequency light using a glass blue short-pass filter and a monochromator, and detected using a photomultiplier tube (PMT). The PMT signal, typically corresponding to 3−10 photons collected per laser shot, was time-gated at a 1 kHz repetition rate triggered by the Pockels cell driver of the Ti: sapphire system, then boxcar averaged. This 1:10^5 duty cycle detection system allows SHG signal collection practically free of the dark current noise. The polarization of the doubled idler laser light, which served as the probe beam, was verified to be better than 100:1, and its polarization was controlled using a half-wave plate. For the molecular orientation measurements, the polarization of the second harmonic signal was analyzed
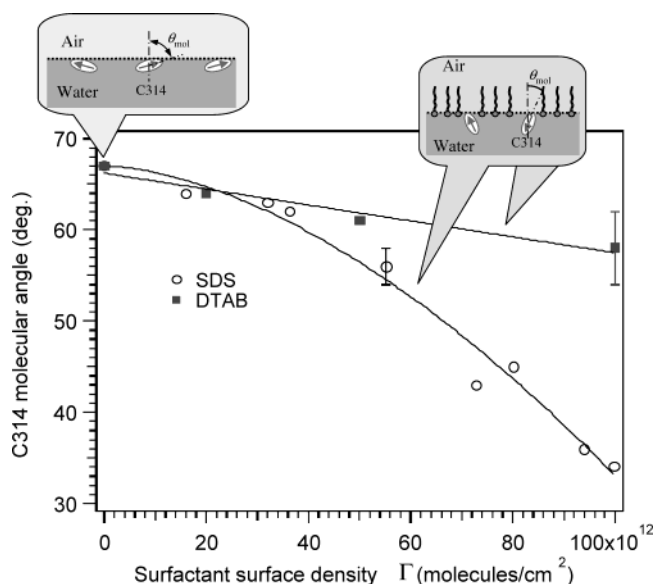
using a broadband Glan-laser polarizer placed in the beam path after the sample.

A small portion of the fundamental output was frequency doubled to produce pump pulses at $\lambda_{pu} = 420$ nm with energy <1 μJ/pulse. The pump−probe delay was controlled using an optical delay line equipped with a stepper-motor driven translation stage. The two beams were overlapped at the sample surface, where the spot size of the pump beam was ~0.5 mm, whereas the probe beam was focused to 150 μm. The pump and probe beams were both 70° from the surface normal but are recombined at a 4° angle in the horizontal plane. This enabled spatial filtering of the SH signal from the reflected pump beam after the sample using four iris apertures. The beaker was rotated at 4 rpm with the pump and probe beams focused 1−1.5 cm off center to avoid local heating, thermal desorption, and bleaching of the C314 adsorbant by the single-photon resonant pump beam.

Results and Discussion

Average molecular orientation of the C314 probe molecules at the DTAB air/water interface was calculated from the SHG null angle measurements.[17] The derivation assumes a narrow orientational distribution of the chromophore transition dipole vectors at the interface. In coumarin 314, the $S_1 \leftarrow S_0$ transition dipole vector μ_{ge} probed by the resonant SHG ($\lambda_{SH} = 430$ nm) is parallel to the permanent dipole moment in the ground state $\mu_g = 8.2$ D, both of which are along the longer axis of the molecule.[18] Figure 3 shows the effect of the positively charged DTAB surfactant film on the orientation θ_{mol} of C314 with respect to the surface normal. The results indicate that the C314 molecules become increasingly aligned more perpendicular to the interface as the surface coverage of the positively charged surfactant increases. This may be an indication of the alignment of the C314 permanent dipole along the electric field lines of the charged plane. Similar behavior was also observed in the alignment of C314 as the anionic SDS surfactant density was increased.[6] However, the orientation change is less pronounced for the positively charged surfactant interface, compared with the negatively charged interface: a $\Delta\theta_{mol} \sim 7°$ change in the C314 angle is observed at the 100 Å^2/molecule DTAB mono-

layer compared to a $\Delta\theta_{mol} \sim 30°$ change for the SDS monolayer of the same surface density. For this comparison, a narrow orientation distribution is assumed. With respect to the orientation of C314, electrostatic considerations point to C314 being oppositely oriented at the positively versus negatively charged surfactant interface. The observed difference in the effects of the positively charged surfactants on the C314 adsorbate orientation suggests that this process is more complex than a simple alignment of the C314 permanent dipole along the field. The differences in the interactions of C314 with the positively charged DTAB/water interface versus the negatively charged SDS/water interface are seen not only in C314 orientation but also in the effect of C314 on the surface pressure versus surface coverage phase diagram, Figure 1C versus Figure 2. The C314 induced change in the DTAB phase diagram is small whereas it causes a large change in the SDS phase diagram. In the case of DTAB, coumarin 314 does not significantly change the saturated monolayer coverage, $\sim$40 $Å^2$/molecule. On the contrary, in the case of SDS, the saturated monolayer coverage was shifted from 48 $Å^2$/SDS molecule in the absence of coumarin to 80 $Å^2$/SDS molecule for 15 μM C314 aqueous solution (Figure 2).

To characterize static solvation at the surfactant-modified air/water interfaces, we measured the solvatochromic shift of the $S_1 \leftarrow S_0$ transition of C314 adsorbed at the positively charged DTAB surfactant interface using steady-state second harmonic generation spectroscopy.[5] Figure 4 compares the SHG spectrum of C314 at the trimethylammonium (DTAB) interface with C314 at the negatively charged surfactant (sodium dodecyl sulfate, SDS) interface of similar coverage. Also shown are the SHG spectrum of C314 at the surfactant-free air/water interface and the linear absorption spectrum of C314 in bulk water. The spectra were fitted using a Lorentzian model with a nonresonant background contribution as described in a previous publication.[7] At the DTAB interface at 200 $Å^2$/molecule surface coverage, the C314 transition maximum is $\lambda_{max} = 436 \pm 2$ nm. In contrast, at the neat air/water interface, the C314 transition is peaked at $\lambda_{max} = 423 \pm 2$ nm. The value of $\lambda_{max} = 432 \pm 2$ nm was measured for anionic surfactant sodium dodecyl sulfate (SDS) at the slightly lower surface coverage of 250 $Å^2$/molecule. Another anionic surfactant, ionized stearic acid (carboxylate headgroup), resulted in the transition wavelength shift to $\lambda_{max}=431\pm2$ nm, which is the same as the SDS surfactant, indicating that it is the negative charge and not the structure of the negatively charged headgroups, i.e., carboxylate versus sulfate, that determines the shift.[7] The width of the C314 transition at the cationic surfactant interface (fwhm = 40 nm) is significantly broader than at the previously studied anionic surfactant interfaces (sulfate, fwhm = 19 nm; carboxylate fwhm = 10 nm). It is also broader than the C314 transition at the surfactant-free air/water interface (fwhm = 16 nm) and approaches that of bulk water, fwhm $\approx$ 65 nm. It should be mentioned that the eletrochromic shift due to the presence of charged surfactant is expected to be small. Our calculation shows that the electrochromic shift of C314, $\mu_{ge} = 4$ D, in the interfacial electric field $E \cong 1.1 \times 10^8$ V/m (corresponding to a DTAB surface coverage of 200 $Å^2$/molecule) is of the order of 2 nm, which is within our experimental uncertainty.

The $S_1 \leftarrow S_0$ transition wavelength is a good indicator of the local polarity of the solvent environment of C314 solute. The permanent dipole moment of coumarin 314 increases from 8.2 D for the ground state to $\sim$12 D for the excited state. Therefore, C314 is positively solvatochromic; i.e., it exhibits a red shift in a more polar solvent environment. A good linear correlation
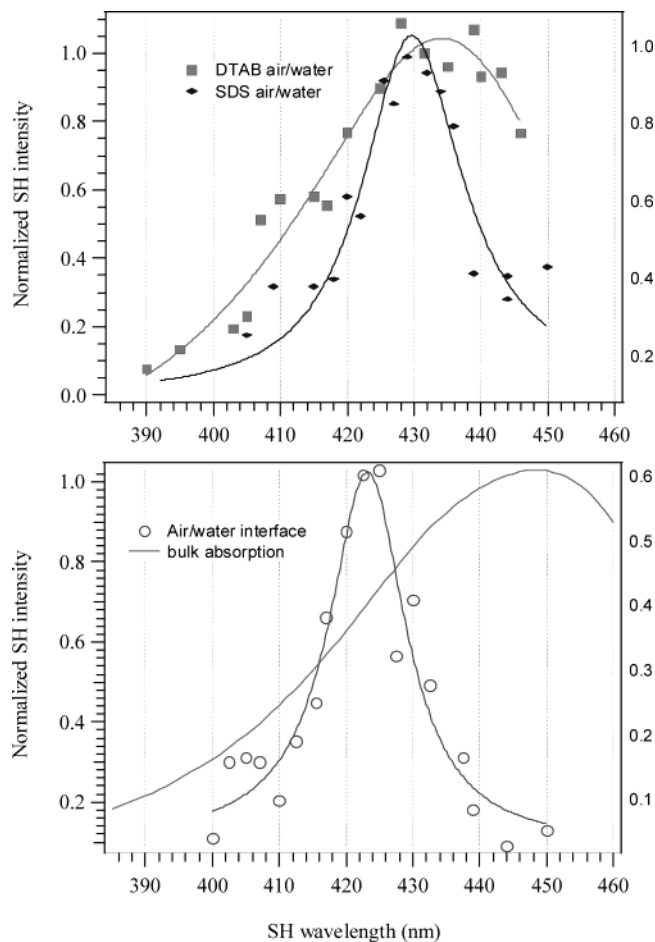

Figure 4. Upper panel: (■) SHG spectra of C314 at the cationic DTAB air/water interface (200 $Å^2$/DTAB molecule); (♦) SHG spectra of C314 at the anionic SDS surfactant air/water interface (250 $Å^2$/SDS molecule). Lower panel: (○) SHG spectra of C314 at the surfactant-free air/water interface. Thin solid line shows the linear absorption spectrum of C314 in bulk water.

has been found between the C314 solvatochromic shift and standard polarity scales of bulk solvent, such as ET(30).[16] From the measurements of the absorption spectra of C314 in various bulk solvents, we found a linear correlation between absorption peak wavelength and ET(30). Using this linear correlation, the ET(30) values of the various interfaces were directly obtained from the measured SHG transition wavelength. In this way, we obtained an ET(30) polarity of 39 for the positively charged DTAB air/water interface at a density of 200 $Å^2$/SDS, and 35 for both the negatively charged SDS air/water interface at a surface coverage of 250 $Å^2$/SDS molecule and the negatively charged stearic acid air/water interface at a surface coverage of 200 $Å^2$/molecule. For comparison, bulk water ET(30) is 63, and the neat air/water interface is 31.

The surface tension measurements (Figure 1C) and the steady-state SHG studies of molecular orientation (Figure 3) and surface spectral measurements (Figure 4) indicate that there is significant interaction between the adsorbed C314 and the surfactants at the interface. The differences observed in surface tension, molecular orientation, and surface spectral results for the DTAB/water interface versus SDS/water interface may be interpreted in terms of different specific interaction of the C314 molecule with the DTAB and SDS headgroups. Another factor that can contribute to these differences is the different orientation of the interfacial water molecules due to the presence of oppositely charged surfactants at the surfaces. Since DTAB and SDS have

Femtosecond Aqueous Solvation

J. Phys. Chem. B, Vol. 108, No. 37, 2004 **14021**

**SCHEME 1: Schematic of C314 Molecules at DATB/Water and SDS/Water Interfaces**
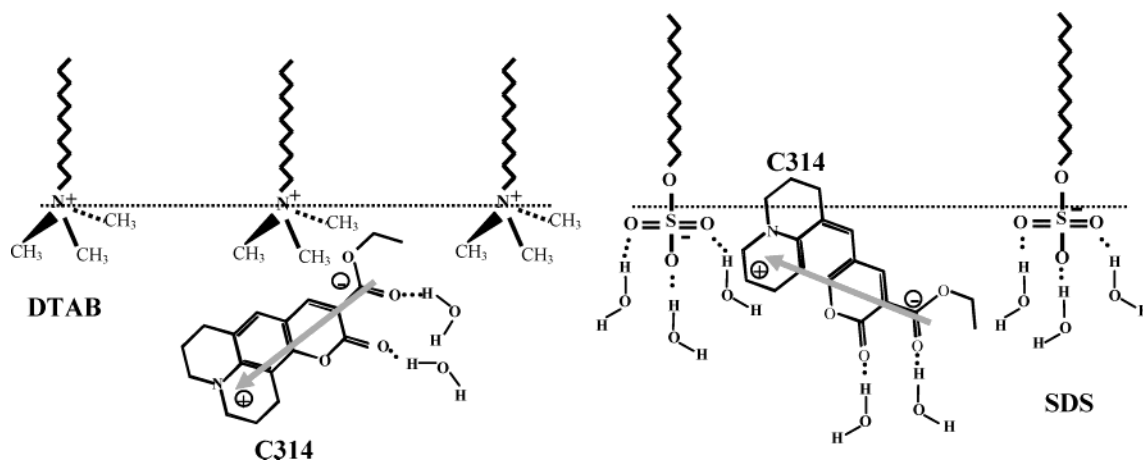
opposite charges, C314 molecules could be oppositely oriented. More specifically, the more negatively charged part of C314 (i.e., the part with oxygen atoms) is likely to point toward the positively charged $N^+(CH_3)_3$ group in DTAB, whereas the more positively charged part of C314 (i.e., the part with N atom) is likely to get in close contact with the negatively charged OSO_3^- group in SDS.

The less pronounced effect of C314 on the phase diagram of the DTAB/water interface compared with the SDS/water interface suggests that the relative positions of the interfacial C314 are quite different for the two different types of surfaces. At the DTAB/water interface, if the interfacial C314 molecules are located below the DTAB surfactant headgroup, perhaps due to hydrophobic interactions between the methyl group of the DTAB headgroup with the nonpolar region of C314 molecule, then the presence of C314 would have a smaller effect on the DTAB phase diagram, in agreement with observations, Figure 1. In contrast, at the SDS/water interface, the C314 molecules may be located between SDS headgroups, perhaps because the interaction of the sulfate headgroup would favor hydrogen bonding interactions with interfacial water molecules. The hydrogen bonding carbonyl groups of C314 would orient toward the water molecule side of the interface with the nonpolar part of C314 facing the air side of the interface. In this case, the presence of C314 molecules can occupy significant surface area and therefore would shift the phase diagram significantly to lower density, as is observed in Figure 2. Such a speculation can also be used to explain why the DTAB/water interface is more polar than the negatively charged interfaces. Since C314 molecules are located below the DTAB headgroup with oxygen atoms up, the C314 molecules are further from the interface, and the static solvation energy is closer to the bulk water value. These considerations would also explain the broader spectral width of C314 at the DTAB/water versus SDS/water interfaces because the possible water configuration about C314 would be closer to that in bulk water, where the spectral width is large (Figure 4). In addition, this description would predict that the C314 orientation would undergo a smaller change as the density of DTAB was increased compared with the large change to be expected when the C314 located closer to the interface is squeezed by increasing the density of SDS. For clarity, the proposed molecular pictures about the location of the interfacial C314 in the presence of DTAB and SDS are shown in Scheme 1.

In addition, as noted earlier, DTAB and SDS affect the orientation of interfacial water molecules in different ways. First, positively charged DTAB can align the surrounding water

molecules with oxygen pointing toward its headgroup, whereas at the SDS/water interface the hydrogen in water molecules point toward the SDS headgroups due to their negative charges. Second, the specific interactions of water molecules with DTAB and SDS are different. There is no hydrogen bonding between water molecules and the methyl groups of the DTAB headgroup. However, there is hydrogen bonding between water molecules and the oxygens of the SDS headgroup.

Femtosecond time-resolved second harmonic generation spectroscopy was employed to characterize solvation dynamics of C314 at the surfactant interfaces. Using the large change of the probe molecule's permanent dipole moment upon electronic excitation, S_1 ($\mu_e = 12$ D) $\leftarrow$ S_0 ($\mu_g = 8.2$ D), the dynamics were initiated by a single-photon resonant pump pulse at $\lambda_{pu} = 420$ nm. The temporal evolution of the resonantly enhanced surface nonlinear optical susceptibility $\chi^{(2)}(t)$ was then monitored by measuring SHG intensity from a time-delayed probe pulse $\lambda_{pr} = 860$ nm ($\lambda_{SH} = 430$ nm). The resulting pump–probe transient SHG signals are shown in Figures 5–7 as a function of the pump–probe delay for the 3 different monolayer densities of the cationic DTAB surfactant, 500, 200, and 100 $Å^2$/molecule. The instrument response time constant, arising from the cross-correlation of the single-photon pump and the second harmonic probe pulses, is estimated to be $\tau_0 = 170$ fs.
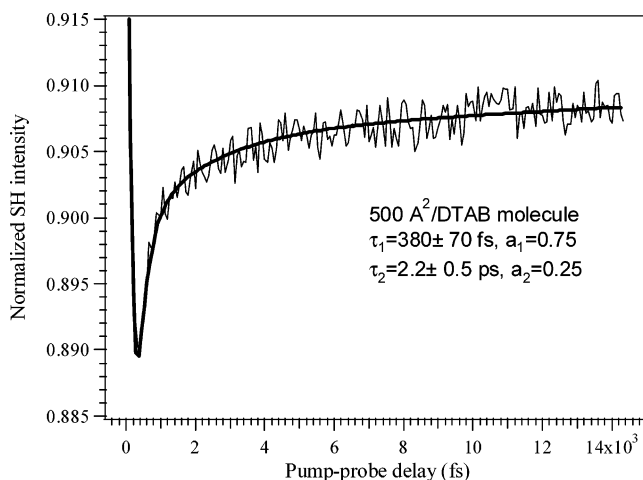
Figure 5. Time-resolved second harmonic generation of the solvation dynamics of coumarin 314 at the DTAB surfactant air/water interface. Bulk concentration of DTAB is 0.14 mM, corresponding to the surface coverage of 500 $Å^2$/DTAB molecule. Thick line shows the fit to the model described in the text, with solvation times of $\tau_1 = 380$ fs and $\tau_2 = 2.2$ ps.
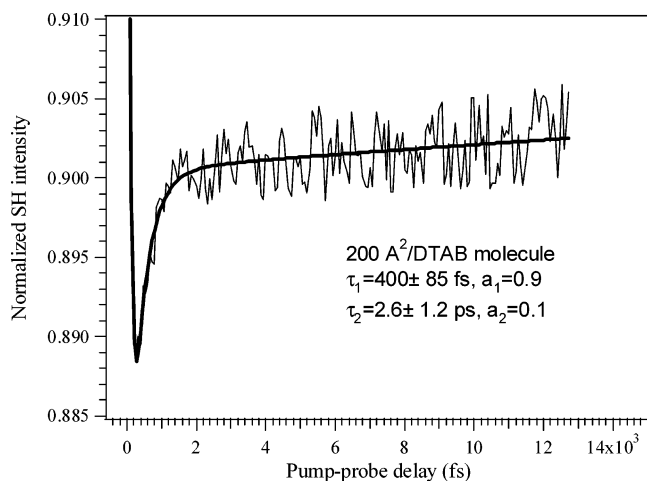
Figure 6. Solvation dynamics of coumarin 314 at the 200 Å²/DTAB molecule air/water interface (bulk DTAB concentration 0.5 mM). Thick line shows the fit to the model described in the text, with solvation times of $\tau_1 = 400$ fs and $\tau_2 = 2.6$ ps.
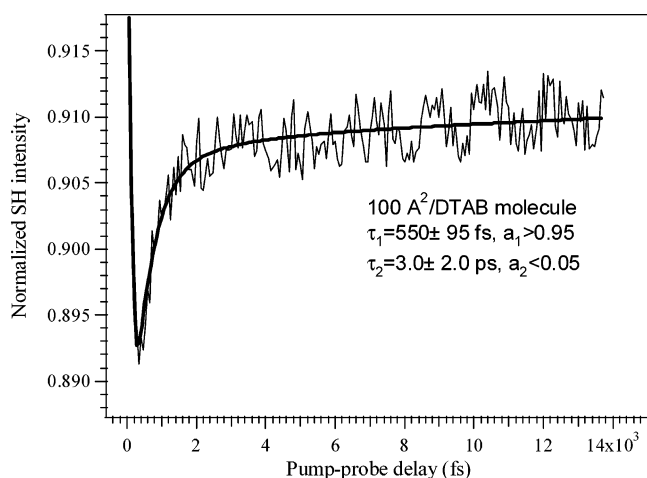
Figure 7. Solvation dynamics of coumarin 314 at the 100 Å²/DTAB molecule air/water interface (bulk DTAB concentration 2.0 mM). Thick line shows the model fit described in the text, with solvation times of $\tau_1 = 550$ fs and $\tau_2 = 3.0$ ps.

Detailed description of the pump−probe TRSHG measurement of the solvation dynamics have been presented eleswhere.[19] Qualitatively, the pump pulse promotes a small fraction (~5%) of the interfacial C314 molecules onto the excited-state potential energy surface. Following the excitation by the pump pulse, the surface nonlinear susceptibility $\chi^{(2)}$ has two resonant contributions, one from the ground-state population n_g and the other from the excited-state population n_e of C314 molecules:

$$\chi^{(2)}(t) = n_g \frac{A_{ge}}{\omega_{ge} - 2\omega + i\Gamma_{ge}} + n_e \frac{A_{eg}}{\omega_{eg}(t) - 2\omega + i\Gamma_{eg}} + B \tag{2}$$

Here, ω_{ge} and Γ_{ge} represent the frequency and spectral widths of the ground-to-excited-state $S_1 \leftarrow S_0$ transition, $\omega_{eg}(t)$ and Γ_{eg} are the corresponding parameters for the excited-to-ground-state $S_1 \rightarrow S_0$ transition, factors A_{ge} and A_{eg} contain the transition matrix elements and nonresonant frequency denominators, and the third term B represents a constant nonresonant contribution. $\omega_{eg}(t)$ is related to the solvation correlation function $S(t)$, which

is used to characterize the solvation dynamics, by

$$S(t) = \frac{\omega_{eg}(t) - \omega_{eg}(\infty)}{\omega_{eg}(0) - \omega_{eg}(\infty)} \tag{3}$$

Solvation of the excited state lowers its energy, thus resulting in the dynamic red shift of the excited-to-ground-state $S_1 \rightarrow S_0$ transition frequency $\omega_{eg}(t)$. Qualitatively, the excited-state solvation shifts the excited-state contribution out of resonance with the SH probe frequency at 2ω, thereby resulting in the time-dependent change of $\chi^{(2)}(t)$. The SH probe wavelength was chosen to be on the blue shoulder of the surface spectrum (430 nm). The model calculation using eqs 2 and 3 shows that in this spectral range the recovery of TRSHG signal $I_{SH}(t)$, which is proportional to $|\chi^{(2)}(t)|^2$, gives a reliable representation of the solvation correlation function $S(t)$; that is, $I_{SH}(t)$ is approximately linearly proportional to $S(t)$.[6,19] In other words, for a model system with realistic spectral parameters, the direct fit of TRSHG data to exponential functions reproduces the time scales of $S(t)$ within 10−15% error. Such a probe wavelength is usually referred to as "linear probe wavelength" in the time-resolved fluorescence Stokes shift measurements.[20,21] For other choices of the SH probe frequency, more complicated SHG dynamics can result.

Solvation dynamics in bulk water[14,15] and at several air−water interfaces[5−7] have been shown to have two exponential components in the subpicosecond to picosecond time window, termed diffusive components. We found that we can fit the experimental data in Figures 5−7 to a two-exponential solvation correlation function

$$S(t) = a_1 \exp(-t/\tau_1) + a_2 \exp(-t/\tau_2) \tag{4}$$

to extract the two diffusive solvation time scales τ_1 and τ_2 and their relative amplitudes a_1 and a_2. The initial decrease in the TRSFG transient signal at $t = 0$ is fit using a convolution of a Gaussian instrument response function with $\tau_0 = 170$ fs, as described in refs 6 and 19. The fitting parameters are summarized in Table 1. For comparison, Table 1 also lists the solvation results for SDS/water and neat air/water interface.

Significant changes in the dynamics are observed as the coverage of the positively charged surfactant increases. At the lowest DTAB coverage, 500 Å²/molecule (Figure 5), two exponential components of solvation dynamics are clearly observed, with time constants $\tau_1 = 380 \pm 70$ fs and $\tau_2 = 2.2 \pm 0.5$ ps and relative intensities $a_1/a_2 \approx 3/1$. These dynamics are similar to the dynamics previously measured at the surfactant-free air/water interface, $\tau_1 = 250 \pm 50$ fs and $\tau_2 = 2.0 \pm 0.4$ ps, $a_1/a_2 \approx 2:1$.[6,16] The faster component slows down to $\tau_1 = 400 \pm 85$ fs at 200 Å²/DTAB molecule (Figure 6), and then to $\tau_1 = 550 \pm 95$ fs at 100 Å²/DTAB molecule (Figure 7). We note that the amplitude of the τ_1 component remains approximately constant as the DTAB surface coverage increases. The slower component, on the contrary, is significantly suppressed in amplitude, to less than 10% for the 200 Å²/DTAB molecule film, and to less than 5% for the 100 Å²/DTAB molecule. This results in significant error bars in the determination of τ_2 from the fit of the data at higher surfactant coverages. The effect of the positively charged surfactant on the solvation dynamics is markedly different from the previously observed dependence of the two dynamical time scales on the negatively charged surfactant coverage.[6] For sodium dodecyl sulfate (SDS), the relative amplitudes of the τ_1 and τ_2 solvation dynamics components remain approximately the same for the SDS surface coverages from 500 to 100 Å² per SDS molecule,

Femtosecond Aqueous Solvation

J. Phys. Chem. B, Vol. 108, No. 37, 2004 **14023**

TABLE 1: Comparison of the Aqueous Solvation Dynamics at Bulk Water, Neat Air/Water, and Positively Charged and Negatively Charged Interfaces

Bulk Water
$\tau_1 = 130-290$ fs ($a_1 = 0.7-03$); $\tau_2 = 0.69-1.2$ ps ($a_2 = 0.3-0.7$)

Air/Water Interface
$\tau_1 = 250 \pm 50$ fs ($a_1 = 0.65$); $\tau_2 = 2.0 \pm 0.4$ ps ($a_2 = 0.35$)

cationic surfactant (DTAB)		anionic surfactant (SDS)[a]	
500 Å^2/DTAB molecule	$\tau_1 = 380 \pm 70$ fs $a_1 = 0.75$ $\tau_2 = 2.2 \pm 0.5$ ps $a_2 = 0.25$	500 Å^2/SDS molecule	$\tau_1 = 270 \pm 50$ fs $a_1 = 0.75$ $\tau_2 = 4.4 \pm 0.9$ ps $a_2 = 0.25$
200 Å^2/DTAB molecule	$\tau_1 = 400 \pm 85$ fs $a_1 = 0.90$ $\tau_2 = 2.6 \pm 1.2$ ps $a_2 = 0.1$	250 Å^2/SDS molecule	$\tau_1 = 225 \pm 25$ fs $a_1 = 0.75$ $\tau_2 = 5.2 \pm 0.6$ ps $a_2 = 0.25$
100 Å^2/DTAB molecule	$\tau_1 = 550 \pm 95$ fs $a_1 > 0.95$ $\tau_2 = 3.0 \pm 2.0$ ps $a_2 < 0.05$	100 Å^2/SDS molecule	$\tau_1 = 600 \pm 70$ fs $a_1 = 0.70$ $\tau_2 = 5.4 \pm 1.1$ ps $a_2 = 0.30$

[a] Data from ref 6.

but the time scales τ_1 and τ_2 change as a function of the anionic surfactant density.[6]

Solvation of a dipolar solute such as C314 in water, which is one of the more polar solvents, is dominated by electrostatic dipole−dipole and hydrogen bonding interactions. The process of aqueous solvation therefore involves translational and rotational motion of water molecules and is intimately connected with the structure and dynamics of the water hydrogen bond network. Our results indicate that the cationic surfactant film significantly affects both static and dynamic solvation of the probe molecule C314 at the air/water interface. This suggests that the water hydrogen bond network near the interface is altered by the interactions with the surfactant headgroups. In the case of the DTAB surfactant, these may include the electrostatic interactions with the positive charge localized on the nitrogen atom and hydrophobic interactions with the methyl groups which may result in formation of clathrate-type structures of water surrounding the trimethylammonium headgroup.

The effects of interfacial charge on the structure of water, as indicated by the second harmonic spectra and solvation dynamics, are observed also in the studies of metal electrodes by X-ray scattering[22,23] and surface-enhanced FTIR spectroscopy.[24,25] These latter studies showed the alignment of water molecules at the charged interfaces. Direct evidence for changes in the hydrogen bonding structure near the charged interface associated with this alignment has been obtained using vibrational sum frequency generation spectroscopy of water at a charged quartz surface[12,26−29] and charged surfactant monolayers at the air/water interface.[9,28] This more highly ordered hydrogen bond structure in the presence of charged surfactants can cause the loss of diffusional (rotational and translational) mobility, which is associated with the arrangement, i.e., breaking, of the water−water hydrogen bonds. Therefore, slower solvation is expected. The differences in dynamical solvation of C314 in the presence of positively charged DTAB and negatively charged SDS and stearate, $CH_3(CH_2)COO^-$, amphiphiles can result from different interfacial water orientations and H-bonding patterns induced by the oppositely charged headgroups and different specific interactions of C314 with DTAB, SDS, and stearate.

The survey of the experimental results presented here shows that the positively charged and negatively charged surfactant films have distinctly different effects on orientation and solvation

at the air/water interface. The asymmetry of the interfacial solvation with respect to the sign of the surface charge may have important potential implications for the solvation and reaction dynamics at biomembrane surfaces, which often contain both anionic and cationic groups.

Conclusions

The effects of a positively charged surfactant on the orientation, and static and dynamic solvation of the probe molecule coumarin 314 at the air/water interface, have been experimentally characterized using steady-state and femtosecond time-resolved second harmonic generation spectroscopy. The positively charged trimethylammonium headgroups of dodecyl trimethylammonium bromide (DTAB) cause significant changes in the equilibrium solvation energies of the probe molecule C314, its interfacial orientation, and its solvation dynamics. The red solvatochromic shift of the coumarin 314 transition at the DTAB/water interface indicates increased polarity resulting from interactions with DTAB compared to the surfactant-free air/water interface, but to a lesser extent than the anionic surfactants studied, sodium dodecyl sulfate (SDS) and sodium stearate. Two time scales of the diffusive solvation dynamics have been measured at the cationic DTAB surfactant interfaces. As the surface coverage increases, the faster component becomes longer, increasing from $\tau_1 = 380 \pm 70$ fs at 500 Å^2/molecule to $\tau_1 = 550 \pm 95$ fs at 100 Å^2/molecule without significant change in amplitude. For the slower component, the remarkable change observed as the surfactant density increases is that the amplitude of the slower component τ_2 is suppressed by more than an order of magnitude. Different behavior of the two dynamical components demonstrates that they arise from different types of water motions.

Comparisons between the positively charged and negatively charged surfactant interfaces reveal significant asymmetry of the solvation properties with respect to the sign of the surface charge. The electrostatic forces would tend to align the water molecules in opposite directions at cationic and anionic interfaces. Changes in the hydrogen bonding water structure are sensitive to the electric field at the surface and to local interactions with the headgroups of the surfactant. Another important factor is the alignment of the C314 molecules at the oppositely charged interfaces. Electrostatic interaction between

the C314 dipole moment and the oppositely directed electric fields of the positively and negatively charged interfaces would lead to the C314 molecules having opposite orientation at these interfaces. This asymmetry in the alignment of water molecules and the C314 adsorbates and differences in the interfacial solvation properties in response to the surface charge may have important consequences in equilibria and dynamics of adsorption and charge-transfer reaction at surfaces of biomembranes.

References and Notes

(1) Gennis, R. B. *Biomembranes*; Springer-Verlag: New York, 1989.

(2) Marcus, R. A. *J. Chem. Phys.* **1956**, *24*, 966.

(3) Nandi, N.; Bagchi, B. *J. Phys. Chem. B* **1997**, *101*, 10954.

(4) Nandi, N.; Bhattacharyya, K.; Bagchi, B. *Chem. Rev.* **2000**, *100*, 2013.

(5) Benderskii, A. V.; Eisenthal, K. B. *J. Phys. Chem. B* **2000**, *104*, 11723.

(6) Benderskii, A. V.; Eisenthal, K. B. *J. Phys. Chem. A* **2002**, *106*, 7482.

(7) Benderskii, A. V.; Eisenthal, K. B. *J. Phys. Chem. B* **2001**, *105*, 6698.

(8) Gragson, D. E.; McCarty, B. M.; Richmond, G. L. *J. Phys. Chem.* **1996**, *100*, 14272.

(9) Gragson, D. E.; McCarty, B. M.; Richmond, G. L. *J. Am. Chem. Soc.* **1997**, *119*, 6144.

(10) Matsumoto, M.; Kataoka, Y. *J. Chem. Phys.* **1988**, *88*, 3233.

(11) Goh, M. C.; Hicks, J. M.; Kemnitz, K.; Pinto, G. R.; Bhattacharyya, K.; Heinz, T. F.; Eisenthal, K. B. *J. Phys. Chem.* **1988**, *92*, 5074.

(12) Du, Q.; Superfine, R.; Freysz, E.; Shen, Y. R. *Phys. Rev. Lett.* **1993**, *70*, 2313.

(13) Jimenez, R.; Fleming, G. R.; Kumar, P. V.; Maroncelli, M. *Nature* **1994**, *369*, 471.

(14) Maroncelli, M.; Kumar, V. P.; Papazyan, A. *J. Phys. Chem.* **1993**, *97*, 13.

(15) Maroncelli, M.; Fleming, G. R. *J. Chem. Phys.* **1988**, *89*, 5044.

(16) Zimdars, D.; Eisenthal, K. B. *J. Phys. Chem. B* **2001**, *105*, 3993.

(17) Heinz, T. F.; Tom, H. W. K.; Shen, Y. R. *Phys. Rev. A* **1983**, *28*, 1883.

(18) Moylan, C. R. *J. Phys. Chem.* **1994**, *98*, 13513.

(19) Shang, X. M.; Benderskii, A. V.; Eisenthal, K. B. *J. Phys. Chem. B* **2001**, *105*, 11578.

(20) Barbara, P. F.; Jarzeba, W. *Adv. Photochem.* **1990**, *15*, 1.

(21) Gardecki, J. A.; Maroncelli, M. *J. Phys. Chem. A* **1999**, *103*, 1187.

(22) Toney, M. F.; Howard, J. N.; Richer, J.; Borges, G. L.; Gordon, J. G.; Melroy, O. R.; Wiesler, D. G.; Yee, D.; Sorensen, L. B. *Nature* **1994**, *368*, 444.

(23) Gordon, J. G.; Melroy, O. R.; Toney, M. F. *Electrochim. Acta* **1995**, *40*, 3.

(24) Ataka, K.; Yotsuyanagi, T.; Osawa, M. *J. Phys. Chem.* **1996**, *100*, 10664.

(25) Habib, M. A.; Bockris, J. O. *Langmuir* **1986**, *2*, 388.

(26) Du, Q.; Freysz, E.; Shen, Y. R. *Science* **1994**, *264*, 826.

(27) Du, Q.; Freysz, E.; Shen, Y. R. *Phys. Rev. Lett.* **1994**, *72*, 238.

(28) Gragson, D. E.; Richmond, G. L. *J. Am. Chem. Soc.* **1998**, *120*, 366.

(29) Gragson, D. E.; Richmond, G. L. *J. Phys. Chem. B* **1998**, *102*, 3847.